frontiers | Frontiers in Earth Science

TYPE Original Research
PUBLISHED 28 December 2023
DOI 10.3389/feart.2023.1231694

OPEN ACCESS

EDITED BY
Ruyue Wang,
SINOPEC Petroleum Exploration and Production Research Institute, China

REVIEWED BY
Wenqiang Tang,
Chengdu University of Technology, China
Wei Dang,
Xi'an Shiyou University, China
Yahao Huang,
Yangtze University, China

*CORRESPONDENCE
DaWei Cheng,
chengdawei123@petrochina.com.cn
ChunYu Qin,
qinchy_0416@163.com
Wenbin Tang,
wbtang@cdut.edu.cn,
tangwenbin100@163.com

RECEIVED 30 May 2023
ACCEPTED 25 August 2023
PUBLISHED 28 December 2023

CITATION
Hong H, Qin C, Zhang S, Zhang Z, Wang X, Li N, Cheng D and Tang W (2023), Early–middle Jurassic source to sink evolution and its tectonic significance in the northeastern Sichuan Basin. *Front. Earth Sci.* 11:1231694. doi: 10.3389/feart.2023.1231694

Early–middle Jurassic source to sink evolution and its tectonic significance in the northeastern Sichuan Basin

HaiTao Hong[1,2], ChunYu Qin[1,2]*, ShaoMin Zhang[1,2], ZhiJie Zhang[3], XiaoJuan Wang[1,2], Nan Li[1,2], DaWei Cheng[3]* and Wenbin Tang[4]*

[1]PetroChina Southwest Oil and Gas Field Company, Chengdu, China, [2]Research Institute of Exploration and Development, PetroChina Southwest Oilfield Company, Chengdu, China, [3]PetroChina Research Institute of Petroleum Exploration and Development, Beijing, China, [4]State Key Laboratory of Oil and Gas Reservoir Geology and Exploitation, Institute of Sedimentary Geology, Chengdu University of Technology, Chengdu, China

This paper discusses the sedimentary environment and source supply in the sedimentary area and their coupling relationship through a detailed description of the deposits from the Ziliujing Formation to Shaximiao Formation of the Lower–Middle Jurassic on the Tieshan section in the Dazhou City, northeastern Sichuan Province, through sedimentary characterization, determination of the paleocurrent direction, analysis of heavy minerals, and detrital zircon U–Pb dating. The results show that the Zhenzhuchong Member is sufficiently supplied with detrital sediments and is dominantly composed of fluvial-delta deposits. The Dongyuemiao Member—the first member of the Lianggaoshan Formation—is dominated by lacustrine deposits, with the detrital supply increased initially in the early Lianggaoshan. The second member of the Lianggaoshan Formation suggests a significant increase in detrital supply, with shrunken lake basin and changed paleocurrent direction. The Shaximiao Formation reveals a complete disappearance of the lake basin in the northern Sichuan Basin. The comprehensive analysis on source supply indicates that the change in source property is apparently coupled with the change in the sedimentary environment, both controlled by orogenesis around the basin. It is inferred from the zircon age distribution that the changes in the sedimentary environment and source supply during the late Ziliujing period and the middle and late Lianggaoshan period resulted from the uplifting of the Micangshan Mountain, Dabashan Mountain, and Qinling Mountain, respectively.

KEYWORDS

heavy mineral composition, zircon U–Pb age, paleocurrent direction, Micangshan Mountain, Dabashan Mountain

1 Introduction

The sedimentary basin and orogenic belt are two basic tectonic units in the upper continental crust. They can be studied as a whole to explore the collisional orogeny and its influence on sedimentation processes and environment change from the perspective of geotectonic geology and sedimentology.

The northern margin of the Sichuan Basin is adjacent to the Dabashan and Micangshan structural belts to the north, separated from the EW-trending Qinling orogenic belt, and

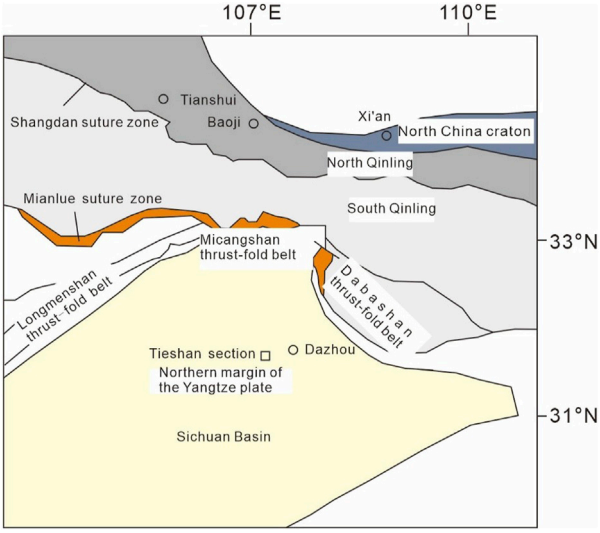

FIGURE 1
Structural sketch of tectonic belts from the northern margin of the Yangtze plate to the North China plate and location of the target section.

bordered by the Songpan–Ganzi and Longmenshan orogenic belts to the west and the Xuefengshan fold belt to the east. It acts as an intersection between multiple structural belts. The Indosinian collision between the Yangtze plate and the North China plate led to a tectonic evolution from the passive continental margin in the northern margin of the Upper Yangtze into the Late Triassic–Early Cretaceous foreland thrust-fold belt and its corresponding foreland basin. The sediments in the northern margin of the Sichuan Basin record the tectonic history of its adjacent orogenic belts. They are ideal for identifying the coupling relationships between the northern margin of the Sichuan Basin and its adjacent orogenic belts.

Many studies have been conducted on the tectonic evolution of sedimentary basin–orogenic belt systems in the northern margin of the Sichuan Basin, including structural interpretation of seismic sections (He et al., 2020), zircon U–Pb dating (Li et al., 2010; Li et al., 2012; Li et al., 2018), and sedimentary environment analysis and paleocurrent direction determination (Qu et al., 2009). However, these studies usually adopted a single method to interpret the tectonic evolution but rarely dealt with sediment–structure coupling; moreover, the interpretation results are different significantly from method to method. On the basis of previous achievements, this paper attempts to explore the uplifting stages of orogenic belts around the basin and their tectonic–sedimentary response relations, through a detailed dissection of field outcrops and the comparison of sedimentary environments and source supply in different periods within the basin.

2 Geological setting

The northeastern Sichuan Basin, i.e., the northeastern margin of the Sichuan Basin, is located in the part transiting from the present-day Qinling orogenic belt to the Sichuan Basin (Figure 1). The Qinling orogenic belt, in the north of the Sichuan Basin, is characteristically composed of three plates and two suture zones. Fu (2016) from north to south, the North China plate, the Qinling micro-plate, and the Yangtze plate are separated by the Shangdan suture zone (Xinyang–Shucheng fault) in the north and the Mianlue suture zone (Xiangfan–Guangji Fault) in the south (Zhang et al., 2001; Wang et al., 2019; Cai, 2020). Structurally, the northeastern Sichuan Basin is connected to the Qinling orogenic belt through the Dabashan thrust-fold belt to the north and the Micangshan thrust-fold belt to the northwest. The northeastern Sichuan foreland basin is a product of the isostatic adjustment induced by huge load of the overthrust sheets under the extrusion stress regime when the South China plate collided with the Qinling micro-plate and North China plate during the late Indosinian and the Central Sichuan land mass subducted into the land beneath the Qinling Mountain in the Yangtze area during the Yanshanian (Li et al., 2012). During the Middle–Late Triassic, along with the closing of the Mianlue Ocean and the emergence of the Qinling orogenic belt, marine sedimentation in the major part of the Sichuan Basin ended and the continental clastic sediments began to deposit in the Late Triassic Xujiahe Formation. The Jurassic continental clastic sediments in the basin, from bottom to top, are composed of the Lower Jurassic Ziliujing Formation (J_1z), which is subdivided into the Zhenzhuchong, Dongyuemiao, Maanshan, and Daanzhai members, the Middle Jurassic Lianggaoshan Formation (J_2l) (also known as the Qianfoya Formation and Xintiangou Formation due to sedimentary facies variation within the basin) and Shaximiao Formation (J_2s), and the Upper Jurassic Suining Formation (J_3s) and Penglaizhen Formation (J_3p) (Yang et al., 2022).

2.1 Sample testing methods

Heavy mineral analysis and isotope dating analysis were conducted on 12 siltstone and fine sandstone samples taken from six intervals in the Dongyuemiao Member, the Daanzhai Member, and the first, second, and third members of Lianggaoshan Formation and the Shaximiao Formation.

Identification and content measurement of heavy minerals and LA-ICPMS zircon U–Pb dating were completed in the State Key Laboratory of Continental Dynamics, Northwest University. The heavy minerals of the rock samples were quantitatively identified and separated by using a binocular microscope and a magnetic separator, through the procedures of screening, rough elutriation, high-intensity magnetic separation, electromagnetic separation, fine elutriation, packaging, and mineral separation. Then, the types of heavy minerals in each sample were statistically determined and the weight ratio of each heavy mineral was calculated. On this basis, the LA-ICP-MS U–Pb dating was performed on the selected zircon grains from some samples. A PVC ring was put on the glass slide, where complete and typical zircon grains were glued with double-faced adhesive tape, and then injected with fully mixed epoxy resin and hardener. The samples were separated from the glass slide when the epoxy resin was solidified fully and then polished until a smooth plane came out. Before measurements, the samples were washed with HNO_3 with a volume percentage of 3% to remove contaminations on the surface. An integration of ICP-MS and the laser ablation system was used for LA-ICPMS zircon U–Pb dating, with a laser beam spot of 32 μm in diameter, 6 Hz, single

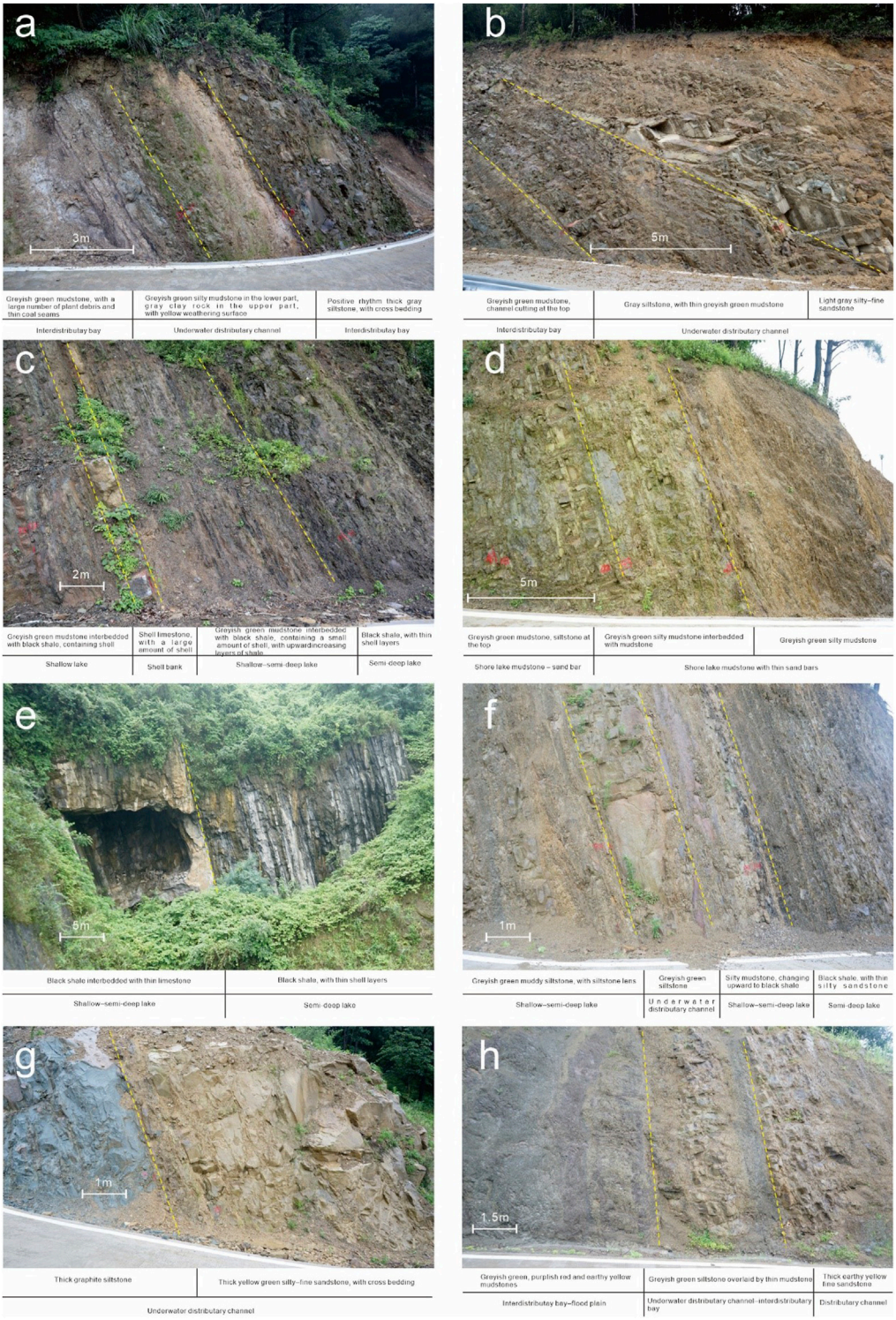

FIGURE 2
Interpretation of the sedimentary environment of intervals on the Tieshan section. **(A, B)** Zhenzhuchong Member, **(C)** Dongyuemiao Member, **(D)** Maanshan Member, **(E)** Daanzhai Member, **(F, G)** Lianggaoshan Formation, and **(H)** Shaximiao Formation.

point ablation, and helium as the carrier gas. Zircon 91500 was measured every five sample points, and standard glass NIST610 and Plesovice zircon were measured every 10 sample points. Each analysis incorporated a background acquisition of 20–30 s (gas blank), followed by 50 s of data acquisition from the sample. ICPMSDataCal was used for offline processing of these analysis data (Liu et al., 2008; Liu et al., 2010a; Liu et al., 2010b). Zircon 91500 served as an external standard for isotope fractionation

correction in the zircon U–Pb dating. Zircon U–Pb concordia diagram mapping and weighted average age calculation were performed by using Isoplot/Ex_ver3 (Ludwig, 2003). The standard deviation of single measurement of the U–Th–Pb isotope ratio, age, and trace elements of zircon was 1σ.

3 Results

3.1 Sedimentary characterization and paleocurrent direction determination

Nearly E–W compression occurred in the eastern Sichuan Basin after the Cretaceous, forming the present SN-trending high and steep fold belt. The Jurassic outcrop in the core of the fold belt provides an ideal stratigraphic section for this study. On the Tieshan section (107.36° E and 31.21° N) to the west of Dazhou City (Figure 1), the strata from the top of the Upper Triassic Xujiahe Formation to the bottom of the Middle Jurassic Shaximiao Formation, with a total thickness of 20 m, are well exposed along a new road through mountains, without any hiatus and huge fault. This study carries out a fine centimeter-scale description of the Tieshan section and records the lithology, color, thickness, sedimentary structure, macroscopic paleontological fossils, and lithofacies superposition of the Lower–Middle Jurassic strata. On this basis, the sedimentary structures indicative of the paleocurrent direction are measured.

On the Tieshan section, the members of the Lower Jurassic Ziliujing Formation exhibit distinctly different sedimentary characteristics with clear interfaces between them. The Zhenzhuchong Member at the bottom is 219 m thick and mainly composed of medium–thin layers of siltstone, grayish-green muddy siltstone, silty mudstone, mudstone, and gray clay rock. It is dominated by delta front facies, and it develops multiple thick layers of underwater distributary channel deposits with trough cross-bedding and parallel beddings, where the deposits of interdistributary bay are mainly fine in grain size with plant debris and coal streaks. The light-gray fine quartz sandstone at the bottom of the Zhenzhuchong Member acts as a parallel unconformity with the underlying gray fine lithic sandstone at the top of the Upper Triassic Xujiahe Formation (Figure 2).

The top of the Zhenzhuchong Member is dominated by light-grayish-green muddy siltstone, and the appearance of black–gray mudstone marks the beginning of the Dongyue Member. The Dongyue Member is 42 m thick and generally lithologically fine. It is mainly composed of medium layers of siltstone, light-gray limestone, black–gray shell-bearing shale, and mudstone. It is believed to be deposited in a shallow–semi-deep lake paleo-environment, where the shallow lake sediments include multiple sand bars and low-energy shell banks, and the semi-deep lake sediments are dominated by low-energy thick shales.

Gray shale is deposited at the top of the Dongyuemiao Member and is covered by gray muddy siltstone at the bottom of the Maanshan Member. The Maanshan Member is 40 m thick and composed of greyish-green mudstone with thin layers of siltstone. It is identified as the deposits of shore lake facies, which include mudflat, beach, and other microfacies.

The appearance of greyish-green shell-bearing silty mudstone followed by the greyish-green mudstone of the Maanshan Member represents the beginning of the Daanzhai Member. The Daanzhai Member is approximately 100 m thick and mainly composed of gray shell limestone and black–gray shell-bearing shale. It is identified as the product of the shallow–semi-deep lake paleo-environment.

After the deposition of gray shell limestone in the Maanshan Formation ended, the Lianggaoshan Formation began with the deposition of thick gray siltstone. The Lianggaoshan Formation is 257 m thick and mainly consists of medium layers of siltstone, greyish-green silty mudstone, mudstone, black–gray shale, and mudstone. It is identified as the deposits of delta front–shallow lake–semi-deep lake facies. The delta front subfacies generally includes multiple underwater distributary channel sand bodies, which are mainly distributed in the upper, lower, and middle parts. According to the latest stratigraphic division proposed by PetroChina Southwest Oil & Gas Field Company, the Lianggaoshan Formation is subdivided into the first, second, and third members from the bottom to top (J_2l_1, J_2l_2, and J_2l_3) roughly by the bottom boundaries of three thick channel sand bodies. J_2l_1 develops the shallow lake deposits in the middle, including shallow lake mudstone, distal sand bar, and beach bar, and is dominated by semi-deep lake shale, shallow lake mud flat, and beach bar at the top. With a significantly increased amount of sand bodies than J_2l_2, J_2l_3 is mainly composed of the shore-shallow lake beach bar, delta front channel, and distal sand bar, with thin layers of lacustrine black and black–gray mudstones.

The Lianggaoshan Formation and Shaximiao Formation are successively deposited, with indistinct boundaries. In this study, the variegated mudstone is considered as the boundary between them. Siltstones alternated with purplish-red/earthy-yellow mudstone and greyish-green mudstone at the bottom of Shaximiao Formation suggest a paleo-environment near the water–atmosphere interface. They are identified as the deposits of delta front–delta plain subfacies. The purplish-red mudstones dominating the middle and upper parts are mainly the deposits of delta plain subfacies, with thick–medium layers of channel fine sandstones (Figures 2, 3).

3.2 Determination of the paleocurrent direction

The Middle–Lower Jurassic deposits in the Tieshan section are generally fine grained. Few indicative sedimentary structures indicative of the paleocurrent direction have been observed, mainly including asymmetric ripples on the surface of sandstone, flute casts at the bottom, and cross-bedding in sandstones. The paleocurrent direction is determined to provide a basis for clarifying the provenance direction, and further research is needed to provide more data. The Zhenzhuchong Member at the bottom indicates the S–W paleocurrent direction (Figures 2, 3). As dominated by shales, the Dongyuemiao and Maanshan members have not provided data for the determination of the paleocurrent direction. The Daanzhai Member indicates that there were multiple paleocurrent directions, including west, south, and southwest, with southwest in dominance (Figures 2, 3). Fluvial sand bodies are deposited at the bottom of the Lianggaoshan Formation (J_2l_1), and the measured paleocurrent directions are dominantly southwest, the same as the Daanzhai

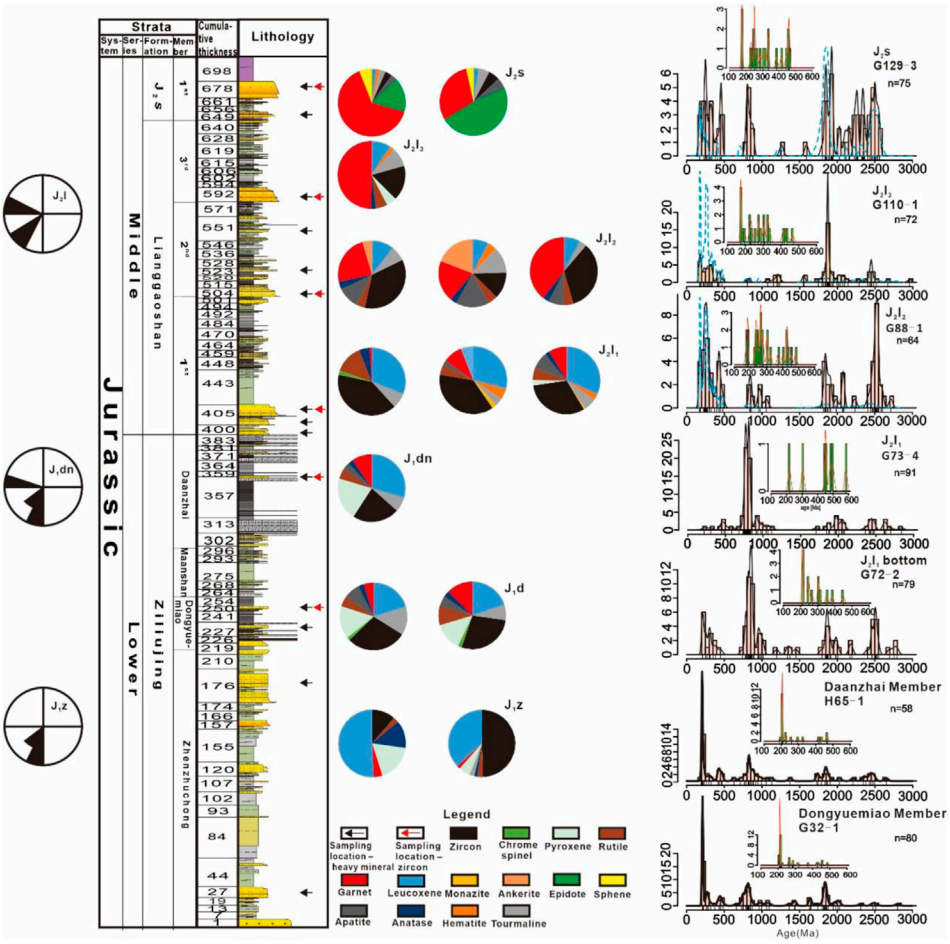

FIGURE 3
Analysis results of paleocurrent direction, lithology, heavy mineral composition, and detrital zircon U–Pb age in the Tieshan section.

Member. The paleocurrent directions measured began to change to southwest and west in the J_2l_2 and J_2l_3 periods, respectively.

3.3 Analysis of heavy minerals

According to the types and proportions of heavy mineral assemblages, a total of five samples from the Zhenzhuchong Member, Dongyuemiao Member, and Daanzhai Member of the Ziliujing Formation show similar characteristics of heavy mineral assemblages. The heavy minerals that account for high proportions include leucoxene, zircon, and pyroxene, and the secondary minerals include rutile, tourmaline, apatite, anatase, and garnet (Figure 2). Differences are also observed between intervals, mainly in the content of secondary minerals. For example, the contents of tourmaline and apatite in the Zhenzhuchong Member are significantly lower than those in the overlying intervals.

Seven samples from the Lianggaoshan Formation are distinct in the heavy mineral assemblage. Three samples from J_2l_1 have similar heavy mineral assemblages that are dominated by leucoxene and zircon, with tourmaline, rutile, apatite, anatase, and garnet (Figure 2).

Four samples from J_2l_2 and J_2l_3 show similar heavy mineral assemblages that are dominated by zircon and garnet, with leucoxene, tourmaline, apatite, rutile, and ankerite (Figure 2).

Two samples from the bottom of J_2l_1 present similar heavy mineral assemblages that are dominated by epidote and garnet, with a small amount of apatite, zircon, tourmaline, and sphene (Figure 2).

3.4 Zircon U–Pb dating

Sample G32-1 from the Dongyuemiao Member of the Ziliujing Formation provided a total of 80 zircon concordia ages, which are divided into five groups (Figure 2). The first group consists of 31 ages in the range of 208–493 Ma. The second group consists of 23 ages in the range of 660–1,098 Ma. The third group consists of three ages in the range of 1,363–1,436 Ma. The fourth group consists of 19 ages in the range of 1,633–2019 Ma. The fifth group consists of four ages in the range of 2,302–2,910 Ma.

Sample H65-1 from the Dongyuemiao Member of the Ziliujing Formation provided a total of 58 zircon concordia ages, which are divided into five groups (Figure 2). The first group is composed of 22 ages in the range of 192–468 Ma. The second group is composed

of 10 ages in the range of 628–1,050 Ma. The third group has only one age of 1,369 Ma. The fourth group is composed of eight ages in the range of 1714–1960 Ma. The fifth group is composed of seven ages in the range of 2,166–2,629 Ma.

Sample G72-2 from the bottom of the Lianggaoshan Formation provided a total of 79 zircon concordia ages, which are divided into seven groups (Figure 2). The first group has 13 ages in the range of 210–447 Ma. The second group has 33 ages in the range of 740–1,046 Ma. The third group has five ages in the range of 1,191–1,450 Ma. The fourth group has 12 ages in the range of 1796–1975 Ma. The fifth group has two ages in the range of 2,140–2,186 Ma. The sixth group has 11 ages in the range of 2,403–2,523 Ma. The seventh group has three ages in the range of 2,697–2,799 Ma.

Sample G73-4 from J_2l_1 provided a total of 91 zircon concordia ages, which are divided into five groups (Figure 2). The first group consists of two ages in the range of 218–303 Ma. The second group consists of five ages in the range of 451–583 Ma. The third group consists of 59 ages in the range of 680–1,123 Ma. The fourth group consists of 13 ages in the range of 1,697–2066 Ma. The fifth group consists of 12 ages in the range of 2,346–2,896 Ma.

Sample G88-1 from J_2l_2 provided a total of 73 zircon concordia ages, which are divided into five groups (Figure 2). The first group has 25 ages in the range of 170–480 Ma. The second group has six ages in the range of 835–1,060 Ma. The third group has 13 ages in the range of 1817–2,220 Ma. The fourth group has 19 ages in the range of 2,397–2,712 Ma. The fifth group has one age of 3,193 Ma.

Sample G110-1 from J_2l_3 provided a total of 72 zircon concordia ages, which are divided into 7 groups (Figure 2). The first group has 22 ages in the range of 173–465 Ma. The second group has one age of 809 Ma. The third group has five ages in the range of 1,076–1,233 Ma. The fourth group has two ages in the range of 1,543–1,553 Ma. The fifth group has 31 ages in the range of 1709–2085 Ma. The sixth group has nine ages in the range of 2,275–2,447 Ma. The seventh group has two ages in the range of 2,654–2,870 Ma.

Sample G129-3 from J_2s_1 provided a total of 75 zircon concordia ages, which are divided into five groups (Figure 2). The first group consists of 20 ages in the range of 173–461 Ma. The second group consists of eight ages in the range of 785–883 Ma. The third group consists of one age of 1,287 Ma. The fourth group has one age of 1,588 Ma. The fifth group consists of 45 ages in the range of 1779–2,587 Ma.

3.5 Comprehensive source analysis

The results of heavy mineral assemblages and zircon U–Pb ages indicate that the northeastern Sichuan Basin has experienced three distinct changes in source supply during the deposition from the Ziliujing Formation to the Shaximiao Formation. They are divided by S_1 (from the end of J_1z to the beginning of J_2l), S_2 (from the end of J_2l_1 to the beginning of J_2l_2), and S_3 (from the end of J_2l to the beginning of J_2s). From above to below S_1, the deposition of the Lianggaoshan Formation started, when the pyroxene content decreased remarkably in mineral assemblages, a small amount of monazite and hematite began to appear, and the proportion of zircons at the Neoproterozoic age began to increase by significant percentages and reached its maximum in the middle of J_2l_1. From above to below S_2, the deposition of J_2l_2 started, when the proportion of garnet increased obviously and the proportion of leucoxene decreased; zircons at the Neoproterozoic age reduced remarkably and almost disappeared in J_2l_3, and the zircons at the Paleoproterozoic and Archean ages increased significantly at the appearance of the Yanshanian zircons (170 Ma). From above to below S_3, the deposition of Shaximiao Formation started, when zircons decreased significantly, epidote and sphene began to be detected, rutile content significantly decreased, zircons at the Neoproterozoic age increased again, and zircons at the Paleoproterozoic and Archean ages continued to increase with a more dispersed distribution.

4 Zircon U–Pb age distribution in potential provenance

The results of paleocurrent direction determination show that the provenances are mainly distributed in the Qinling orogenic belt to the north of the study area. Along with the progress of orogenic chronology, petrographic composition and formation age of each tectonic unit within the Qinling orogenic belt have been gradually clarified (Figure 4). The southern margin of the North China craton mainly has outcrops of the Taihua and Dengfeng groups in the Neoarchean basement, the Paleoproterozoic Angou Group, and the Middle Proterozoic Xionger Group volcanic rocks (Zhang et al., 2000). Three major tectonothermal events occurred in the Early Neoarchean period (2.7–2.9 Ga), Late Neoarchean period (2.2–2.5 Ga), and Middle Paleoproterozoic period (1.8–2.1 Ga) (Zhai et al., 2000). Since the Meso-Cenozoic, a large number of granites formed by the collision between the South China plate and the North China plate have been distributed extensively in the southern margin of the North China plate and the east of the North Qinling orogenic belt. Their zircon ages are mainly concentrated in the Indosinian (~278 Ma) and the Late Caledonian (~463 Ma), and few in the Late Neoproterozoic (~906 Ma) (Figure 5A).

From north to south, the Kuanping Group Complex, Erlangping Group Complex, Qinling Group Complex, Songshugou ophiolite fragment, and Danfeng Group Complex are outcropped successively in the North Qinling orogenic belt. The Kuanping Group Complex was formed during the Neoproterozoic–Early Paleozoic, the Erlang Group Complex was formed in the Early Paleozoic, the Qinling Group Complex was deposited in the Early Neoproterozoic, the Songshugou ophiolite was formed by the Mesoproterozoic tectonic emplacement, and the Danfeng Group Complex was developed in the Late Neoproterozoic (Shi et al., 2013; Dong et al., 2016). Four peaks, 2.4–2.6 Ga (Neoarchean), approximately 850–950 Ma, approximately 744 Ma, and 450–350 Ma (Early Paleozoic), are shown in the distribution of detrital zircon ages of the North Qinling orogenic belt (Figure 5B).

The South Qinling orogenic belt is geologically composed of the Neoarchean–Paleoproterozoic crystalline basement, the Meso-Neoproterozoic transitional basement, and the Paleozoic and Lower–Middle Triassic deposits. Oblique collision between

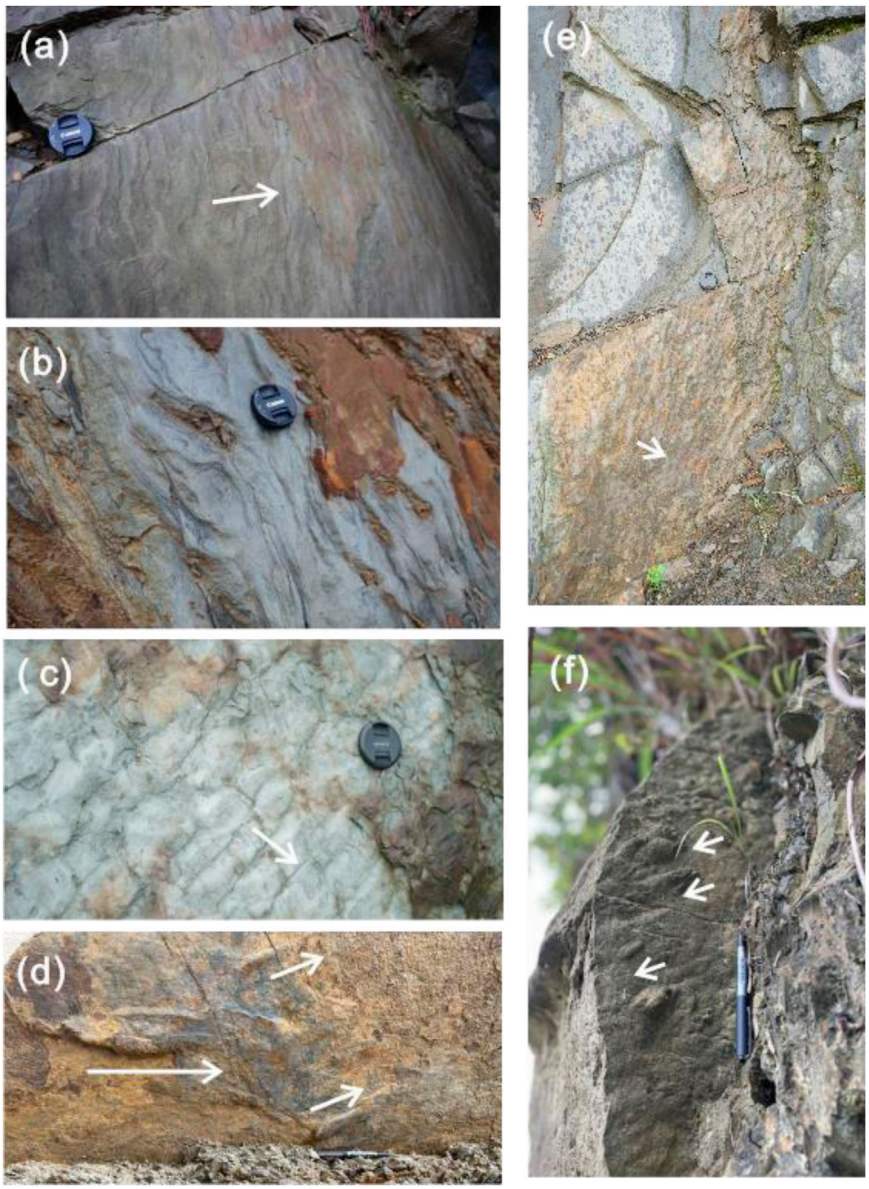

FIGURE 4
Indicated paleocurrent directions. **(A)** Asymmetrical ripple marks in the Zhenzhuchong Member; **(B)** small-scale cross-bedding in the Zhenzhuchong Member; **(C, E)** asymmetrical ripple marks at the bottom of the Daanzhai Member; and **(D, F)** marks on the bottom of the thick fluvial sand body in J_2l_2. The white arrows indicate the flow direction.

the Yangtze plate and the North China plate occurred during the Indosinian, when a large amount of syncollisional volcanic rocks were developed along the Mianlue suture zone, ranging between 206 Ma and 220 Ma in age (Sun et al., 2000; Hu et al., 2004), and granites were developed extensively in Caoping, Zhashui Yangba, and Foping areas with ages peaking at 216 Ma. At the same time, the zircons at the Late Caledonian–Early Hercynian age (~443 Ma) and the Late Neoproterozoic age (~751 Ma) were distributed sporadically in the northern margin of the South Qinling. The Meso-Neoproterozoic transitional basement composed of volcanic–sedimentary rock series is the principal part of the South Qinling basement and is represented by the Wudang Group and Yunxi Group, as well as the Bikou Group, in the west (Ling et al., 2002; Li et al., 2003). The Yudongzi Group of the Neoarchean basement is sporadically exposed near the Lueyang–Ningqiang area and was formed around 2.7 Ga ago (Zhang et al., 2005; Zhang et al., 2010). Zhang et al. (2001) believed that the uplifting of Mianlue suture zone and South Qinling orogenic belt during the Middle–Late Hercynian–Indosinian, when the collisional orogeny of the Qinling–Dabieshan orogenic belt ended, provided abundant sediments to the foreland basin (Figure 5C).

The northern margin of the Yangtze plate mainly refers to the part adjacent to the South Qinling orogenic belt in the south of the Mianlue–Chengkou–Fangxian–Xiangguang Fault, including the Hannan and Micangshan uplifts in the northern margin of

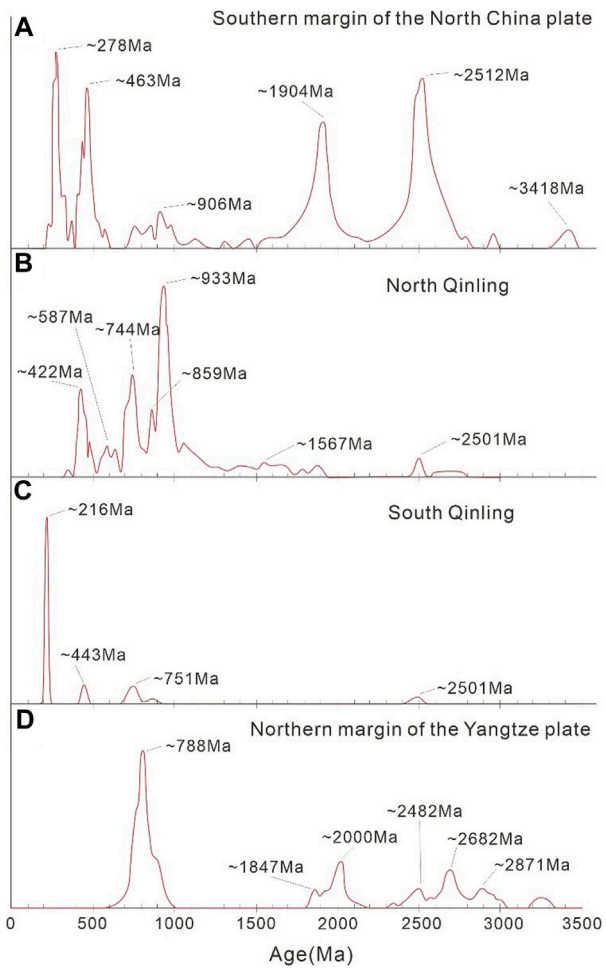

FIGURE 5
Zircon U–Pb age distribution in potential provenance (modified from the work of Qian (2015)).

the Sichuan Basin, where a small amount of Archean basement (e.g., Kongling and Honghe groups) and a large number of Neoproterozoic basement are mainly exposed. Volcanic rocks were barely developed since the Phanerozoic and have three major peaks of zircon age, i.e., ~2,682 Ma, ~2000 Ma, and ~788 Ma (Diwu et al., 2012). Pre-Sinian magmatic and metamorphic rocks are dominantly exposed in the Hannan area, and the Neoproterozoic basic–intermediate-acid intrusive rocks widely exposed near the Xixiang–Hanzhong area are known as the "Hannan Complex." Its formation age was reported as 837–800 Ma (Zhang et al., 2000; Zhao et al., 2006; Zhao et al., 2008; Geng, 2010). Zircon U–Pb dating provides ages of 778 ± 5 Ma for tonalites in the Wudumen composite granite within the Hannan Complex and 840–820 Ma for volcanic rocks of the Sunjiahe Formation in the Hannan area, suggesting a close association between formation of the magmatic rocks and break-up of Rodinia Supercontinent (Dong et al., 2011; Dong et al., 2012). The Proterozoic metamorphic rocks and polyphasic intrusive magmatites and their surrounding Paleozoic and Mesozoic sedimentary rocks are the major part of the Micangshan Mountain (Figure 5D).

5 Comprehensive source analysis

The identified paleocurrent direction from the Zhenzhuchong Member suggests the principal provenance as the North Qinling orogenic belt to the north. The identified multiple paleocurrent directions from the Dongyuemiao and Daanzhai members indicate an input of sediments from multiple directions. Consistent heavy mineral assemblages and highly similar distribution of zircon U–Pb ages were observed within the Ziliujing Formation. The zircon ages are mainly in the range of 205–210 Ma, followed by 750–850 Ma, and few in the ranges of 400–500 Ma, 1700–19000 Ma, and 2,400–2,500 Ma. This zircon age distribution is highly similar to that in the South Qinling area, so the South Qinling is inferred as a provenance for the Ziliujing Formation. A small amount of zircons at the Early Paleozoic and Neoproterozoic ages probably came from the Dabashan Mountain, Hannan area, and Micangshan Mountain on the pathway from the South Qinling to the sedimentary area (Sun, 2014). It reveals low-amplitude uplifting of the Dabashan and Hannan–Micangshan occurred during the Ziliujing period, providing a small amount of sediments to the sedimentary area. Zircon ages of the North Qingling have not been detected, indicating that the South Qingling had been uplifted during this period, which hindered the sediment supply from the North Qinling.

From J_1z to J_2l^1, zircons at the Late Triassic age reduced and those at the Neoproterozoic age increased gradually. The zircon age distribution in the middle of J_2l_1 shows a high consistency to that in the northern margin of the Yangtze craton. Based on the indications of the paleocurrent direction that the sediments mainly came from the north and the Neoproterozoic zircons are currently exposed in the Hannan area and Micangshan Mountain, it is speculated that the Hannan area and Micangshan Mountain that were rapidly uplifted during this period have gradually become the major provenances for the sedimentary area and have hindered the source supply from the South Qingling to the north until the early Lianggaoshan period. Moreover, a small amount of the Early Paleozoic zircons are inferred to originate from the Dabashan Mountain.

In the J_2l_2 period, the paleocurrent direction changed to W–WS from S–SW. Compared with the older formations, J_2l_2 shows a different zircon age distribution. Specifically, the zircons younger than the Mesoproterozoic show a significantly increased proportion and have a greater number than all of the zircons at the Neoproterozoic age, which corresponds to the basement formation stage of the North China plate, Yangtze plate, and Qinling orogenic belt. In addition, a few young zircons at ages (170–180 Ma) approximate to the synsedimentary age appear. Despite having a small number (only 3–5 in each sample), these young zircons have been detected in high concentrations in three samples, confirming the credibility of analysis results. By comparison, it is shown that the zircon ages of $J_2l_{2\text{-}3}$ in the study area and in the Lianghekou area reported by Qian (2015) are centralized in same ranges; however, they have significant differences in their proportions. It is also indicated that the provenance of $J_2l_{2\text{-}3}$ consists of at least two parts: one is composed of relatively younger zircons formed after 400 Ma, and the other is made up of older zircons at age of 400–2,500 Ma. It is speculated the younger zircons came from the South Qinling in the north, and those of older age were transported from the northwest. The older zircons have been recorded in neither the North Qinling

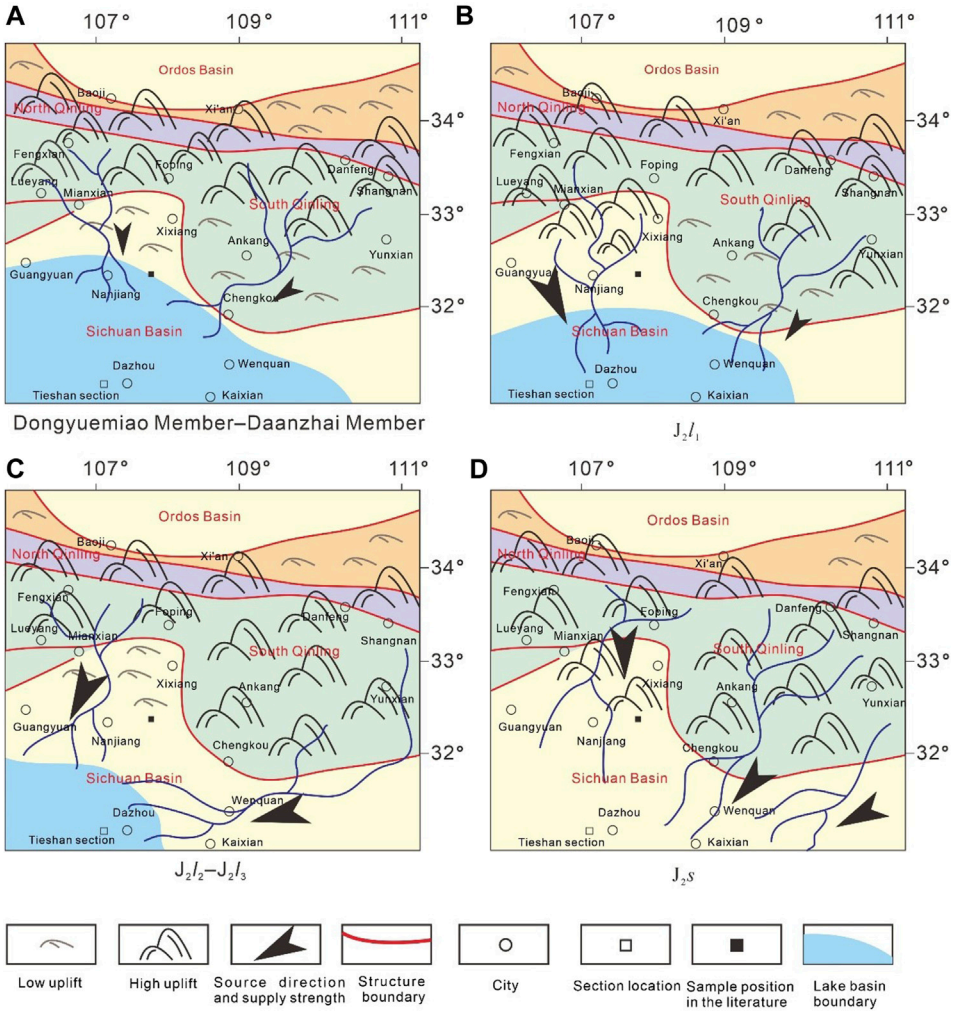

FIGURE 6
Variation in the Middle–Lower Jurassic sedimentary area and provenance in the northeastern Sichuan Basin.

nor the South Qinling, only in the North China plate, resulting in significant controversy on their source. For example, provenance of the Archean–Paleoproterozoic zircons was reported as the ancient basement of the Qingling orogenic belt by Li et al. (2010), was speculated to be the northern margin of the South China plate by Qian (2015), and was indicated as the Paleozoic–Early Mesozoic sedimentary rocks by Li et al. (2018). These zircons show similar age distribution to the southern margin of the North China plate. However, it was impossible for erosion products of the North China plate to break through the barrier formed by the fore-arc accretionary wedges generated by subduction and collision between plates during the Archean–Paleoproterozoic. Therefore, it is concluded that the zircons are mainly from the earlier sedimentary rocks mingled with zircons in the basement of the Qingling orogenic belt. According to the emergence of young zircons and increase of old zircons in this period, an inference could be drawn that the Qingling orogenic belt experienced strengthened tectonic movement during J_2l_2. Consequently, a larger number of old layers and basement rocks cropped out and suffered erosion. In the meanwhile, the rapid uplifting of the Dabashan Mountain allowed an input of sediments in the north from the northeast of the basin and generated a major influence on the northeastern Sichuan Basin and a significantly decreased impact on the northern part of the central Sichuan Basin. Moreover, the remarkably reduced amount of the Neoproterozoic zircons and their gradually decreasing trend from J_2l_2 to J_2l_3 suggest that the Hannan area and Micangshan Mountain have experienced another tectonic stabilization after short-term uplifting followed by deposition of the Ziliujing Formation. Due to long-term denudation, the Hannan area and Micangshan Mountain provided gradually reducing sediments to the sedimentary area.

Zircon age distributions in both the lower J_2s_1 and $J_2l_{2\text{-}3}$ are similar and comparatively more dispersive than other formations. It could be explained by their more complex source and the possible combined contribution of multiple sources. Another increase in the proportion of the Early Paleozoic zircons indicates that the Hannan area and Micangshan Mountain were uplifted again, leading to an increased proportion of the sediments provided by it to the sedimentary area. A comparison of detrital zircons in the Shaximiao Formation between the study area and in the

Kaixian–Wenquan area that was reported by Li et al. (2010) shows similar age distributions. However, the Neoproterozoic zircons have been barely detected in the former, suggesting that the sediments from the Micangshan Mountain failed to extend into Kaixian–Wenquan.

6 Uplifting stages of adjacent orogenic belts and their influence on sedimentary evolution

Along with the closing of the Qingling Ocean, the Sichuan Basin evolved from a marine basin into a continental basin during the Middle–Late Triassic. The sedimentary center migrated from the western Sichuan Basin to the Micangshan Mountain and Dabashan Mountain in the northern Sichuan Basin in the Jurassic (Cheng, 2014). The results of this study indicate that the Early–Middle Jurassic provenance of the northeastern Sichuan Basin mainly includes the northern margin of Yangtze plate and the Qinling orogenic belt and excludes the source supply from the North Qinling orogenic belt. It suggests that tectonic uplifting of the South Qingling orogenic belt occurred in the Early Jurassic. Tectonic activities within the northeastern Sichuan Basin caused the unconformity contact between the Triassic and the Jurassic, and the subsequent uplifting and denudation continued until the Early Jurassic, when the deposition of the Zhenzhuchong Member ended. The subsequent tectonic stabilization allowed a change from fluvial-delta facies with strong sediments supply to lacustrine facies in the northeastern Sichuan Basin (Figure 6A).

There is still a relatively large controversy on the uplifting period of the Micangshan Mountain in the northern Sichuan Basin. According to the distribution of continental sequences, it is generally believed that the Micangshan Mountain experienced large-scale uplifting in the Late Triassic and another intensive uplifting under the action of the Longmenshan Mountains and Qingling Mountains in the Early Jurassic; after that, slow uplifting continued until overthrusting occurred during the Himalayan (Guo, 1996; Liu et al., 2003). Based on the internal unconformities in the Triassic strata, Shen et al. concluded that the Micangshan Mountain had developed thrust belts in the Early Triassic, and the front of thrust belts had reached the present front of the foreland thrust belt (Shen et al., 2010). The recent apatite fission track analysis and zircon (U–Th)/He dating indicate that the Micangshan Mountain experienced rapid uplifting and relative large-scale erosion in the late Early Cretaceous and another rapid uplifting at 20–15 Ma. The apatite fission track data of the Micangshan structural belt show that it is generally younger than the Sichuan Basin in the north and reflect that uplifting of the thrust belt and uplifting of the basin are not synchronous processes, with the former occurring earlier. The Micangshan Mountain was dominated by sedimentation due to generally weak tectonic effect before the Cretaceous, experienced intensive intracontinental deformation and mainly finalized structurally during the Cretaceous, and has been uplifted as a whole since the Late Eocene. Through dating the zircons from clastic rocks in front of the Micangshan Mountain, Li et al. analyzed the change in source supply of the southern margin of the Micangshan Mountain since the Late Triassic. It was speculated that the Hannan–Micangshan area experienced uplifting and erosion in the Late Triassic, followed by piggy-back uplifting to the south of the South Qingling orogenic belt in the Early Jurassic, which continued to the Late Jurassic; during the Early Cretaceous, the front of the Micangshan Mountain accepted sediments from multiple provenances along with intensive orogenic movement within the peripheral orogenic belts of the Sichuan Basin (Li et al., 2018). He et al. reported two stages in the tectonic evolution of the Micangshan Mountain: the late Early Cretaceous–early Late Cretaceous slip deformation and the Neogene large-scale uplifting (He et al., 2020). According to the results of this study, it is considered that the Micangshan Mountain was not exposed dramatically in the Early Jurassic but was probably uplifted slightly and stabilized tectonically again after one stage of rapid uplifting (Figure 6B). As it lasted for a short time, the uplifting mainly provided a large amount of clastic sediments to the study area but failed to change its characteristic dominance of lacustrine sediments.

Many scholars have worked a lot on the tectonic evolution of the Dabashan Mountain. Xie regarded the Dabashan Mountain as the product of superposition of two stages of tectonic processes: the earlier stage is the Indosinian collision orogenesis in the south of the South Qinling (230–200 Ma), which is the dominant controlling tectonic event; and the later stage is the Late Indosinian–Early Yanshanian extensional collapse and the intracontinental orogenesis in the Middle–Late Yanshanian (165–100 Ma) (Xie et al., 2014). He et al. divided the tectonic evolution of Dabashan Mountain into four stages: 1) during the Middle–Late Triassic, the northern Dabashan Mountain was formed and the southern Dabashan Mountain was still located in the subsidence center; 2) during the Late Triassic to Early Jurassic, the northern Dabashan Mountain mainly experienced thrusting and was uplifted as a whole; 3) during the late Early Cretaceous, the northern Dabashan Mountain was fully formed, and the southern Dabashan Mountain began to thrust, resulting in a wide and gentle anticline cropped out; and 4) during the Paleogene, the southern Dabashan Mountain started to suffer a strong deformation (He et al., 2020). The results of this study indicate that the Dabashan Mountain experienced low-amplitude uplifting during the Early Jurassic and rapid uplifting during J_2l_2 (Figure 6C). The rapid uplifting of Qinling and Dabashan Mountains supplied a large amount of sediments to the basin and also changed their input direction, and the extensive shrinkage of lake basin in the northeastern Sichuan Basin changed the sedimentary facies characterized by the lacustrine deposits in dominance that have been formed since the end of Zhenzhuchong Member deposition.

A large-scale tectonic compression in the Qingling orogenic belt during the deposition of the Shaximiao Formation further uplifted the Dabashan and Micangshan mountains, which provided a significant amount of sediments to the foreland basin, and lake basins disappeared completely in the northeastern Sichuan Basin (Figure 6D).

7 Conclusion

The strata from the Ziliujing Formation to the bottom of the Shaximiao Formation on the Tieshan section and the northwestern Sichuan Basin suggest the paleocurrent direction generally as NE–SW.

(1) The Zhenzhuchong Member is sufficiently supplied with detrital sediments and is dominantly composed of fluvial-delta deposits. The Dongyuemiao Member–J_1l_1 is dominated by lacustrine

deposits. An enhanced source supply has been detected from the end of Daanzhai Member to J_1l_1. Since the initial deposition of J_1l_2, the detrital supply increased and lake shrinkage occurred. The detrital supply reached its maximum during the deposition of the Shaximiao Formation when the lake basin disappeared completely in the northern Sichuan Basin.

(2) The heavy mineral assemblages and zircon U–Pb ages indicate that the northeastern Sichuan Basin has experienced three distinct changes in source supply, respectively, between the Ziliujing period and the Lianggaoshan period, between J_2l_1 and J_2l_2, and between the Lianggaoshan period and the Shaximiao period. The latter two are the most distinct.

(3) The sediments of the Ziliujing Formation were mainly sourced from the South Qingling, and the source supply from the Hannan and Micangshan Mountain increased rapidly during the J_2l^2 deposition. The source properties were complicated when the Shaximiao Formation was deposited, with the combined contribution of multiple provenances detected.

(4) Changes in the sedimentary environment and source supply are responses to tectonic activities. The three changes in the study area correspond to the uplifting of the Micangshan Mountain, the uplifting of the Dabashan Mountain, and the overall uplifting of the Qinling orogenic belt, respectively. Along with the three phases of tectonic uplifting, lake basins gradually shrank and finally disappeared completely in the northeastern Sichuan Basin.

Data availability statement

The datasets presented in this study can be found in online repositories. The names of the repository/repositories and accession number(s) can be found in the article/Supplementary Material.

Author contributions

HH: Conceptualization, Methodology, Writing-Original Draft. CQ: Conceptualization, Methodology, Writing-Original Draft. SZ: Data curation, Supervision. ZZ: Supervision. XW: Supervision. NL: Formal analysis. DC: Investigation. WT: Validation.

Funding

This research was supported by the Natural Science Foundation of China (NSFC) Project (No. 42202188), and TW was supported by the Sichuan Science and Technology Program (No. 2023NSFSC1986).

Conflict of interest

HH, CQ, SZ, XW, and NL were employed by PetroChina Southwest Oil and Gas Field Company, PetroChina Southwest Oilfield Company. ZZ and DC were employed by PetroChina Research Institute of Petroleum Exploration and Development.

The remaining author declares that the research was conducted in the absence of any commercial or financial relationships that could be construed as a potential conflict of interest.

The reviewer WT declared a shared affiliation with the authors WT, XK to the handling editor at time of review.

Publisher's note

All claims expressed in this article are solely those of the authors and do not necessarily represent those of their affiliated organizations, or those of the publisher, the editors, and the reviewers. Any product that may be evaluated in this article, or claim that may be made by its manufacturer, is not guaranteed or endorsed by the publisher.

References

Cai, R. (2020). Detrital records of the eastern qinling indosinian orogenic processes: sedimentology and sedimentary provenance analysis of the middle triassic-early jurassic successions in zigui basin. PhD dissertation. Beijing: China University of Geosciences.

Cheng, L. X. (2014). Sedimentary response within orogenic movement of basin edge during late triasiic to jurassic in eastern and northern sichuan, China. PhD dissertation. Chengdu, China: Chengdu University of Technology.

Diwu, C. R., Sun, Y., Zhang, H., Wang, Q., Guo, A. L., and Fan, L. G. (2012). Episodic tectonothermal events of the western north China craton and North Qinling orogenic belt in central China: constraints from detrital zircon U-Pb ages. *J. Asian Earth Sci.* 47 (3), 107–122. doi:10.1016/j.jseaes.2011.07.012

Dong, Y. P., Liu, X. M., Santosh, M., Chen, Q., Zhang, X. N., Li, W., et al. (2012). Neoproterozoic accretionary tectonics along the northwestern margin of the Yangtze block, China: constraints from zircon U-Pb geochronology and geochemistry. *Precambrian Res.* 196-197, 247–274. doi:10.1016/j.precamres.2011.12.007

Dong, Y. P., Liu, X. M., Santosh, M., Zhang, X. N., Chen, Q., Yang, C., et al. (2011). Neoproterozoic subduction tectonics of the northwestern Yangtze block in South China: constrains from zircon U-Pb geochronology and geochemistry of mafic intrusions in the hannan massif. *Precambrian Res.* 189, 66–90. doi:10.1016/j.precamres.2011.05.002

Dong, Y. P., Yang, Z., Liu, X. M., Sun, S. S., Li, W., Cheng, B., et al. (2016). Mesozoic intracontinental orogeny in the qinling mountains, central China. *Gondwana Res.* 30 (1), 144–158. doi:10.1016/j.gr.2015.05.004

Fu, J. H. (2016). *Late paleozoic-mesozoic basin evolution in the longmenshan-dabashan region and its tectonic implications*. Thesis (Beijing: China University of Geosciences).

Geng, Y. Y. (2010). SHRIMP zircon U-Pb dating and geochemical characteristics of granites in the northern margin of the Yangtze block. master dissertation. Beijing: China University of Geosciences.

Guo, Z. W., Deng, K. L., and Han, Y. H. (1996). *Formation and evolution of Sichuan Basin*. Beijing: Geological Press, 120–138.

He, D. F., Li, Y. Q., Huang, H. Y., Zhang, J., Lu, R. Q., and Li, D. (2020). *Formation, evolution and hydrocarbon accumulation of multi-cycle superimposed basins in sichuan.* Science Press, 49–83.

Hu, J. M., Cui, J. T., Meng, Q. R., and Zhao, C. Y. (2004). Zircon U-Pb age of the Zhashui pluton in Qinling Mountains and its geological significance. *Geol. Rev.* 50 (3), 323–329.

Li, H. K., Lu, S. N., Chen, Z. H., Xiang, Z. Q., Zhou, H. Y., and Hong, G. J. (2003). Zircon U-Pb geochronology of rift-type volcanic rocks of the yaolinghe group in the South qinling orogen. *Geol. Bull. China* 22 (10), 775–781.

Li, J. H., Zhang, Y. Q., Xu, X. B., Dong, S. W., and Li, T. D. (2012). Zircon U-Pb LA-ICP-MS dating of fenghuangshan pluton in northern dabashan mountains and its implications to tectonic settings. *Geol. Rev.* 58 (2), 581–593.

Li, R. B., Pei, X. Z., Liu, Z. Q., Li, Z. C., Ding, S. Q., Liu, Z. G., et al. (2010). Basin-mountain coupling relationship of foreland Basins between dabashan and northeastern sichuan-the evidence from LA-ICP-MS U-Pb dating of the detrital zircons. *Acta Geol. Sin.* 84 (8), 1118–1134.

Li, S. J., Sun, D. S., Cai, L. G., Gao, P., and Li, T. Y. (2018). Detrital zircon U-Pb geochronology of Micangshan Mountain piedmont zone, northern sichuan Basin and its significance to basin-mountain evolution. *Geotect. Metallogenia* 42 (6), 1087–1107.

Ling, W. L., Gao, S., Oyang, J. P., Zhang, B. R., and Li, H. M. (2002). Age and tectonic setting of the Xixiang group: constraints on isotopic chronology and geochemistry. *Sci. China (Series D)* 32 (2), 101–112.

Liu, S. G., Luo, Z. L., and Zhao, X. K. (2003). Coupling relationships of sedimentary basinbasin-orogenic belt systems and their dynamic models in west China-A case study of the longmenshan orogenic belt- west sichuan foreland basin system. *Acta Geol. Sin.* 77 (2), 177–186.

Liu, Y., Gao, S., Hu, Z., Gao, C., Zong, K., and Wang, D. (2010a). Continental and oceanic crust recycling-induced melt-peridotite interactions in the trans-north China orogen: U-Pb dating, Hf isotopes and trace elements in zircons from mantle xenoliths. *J. Petrology* 51 (1), 537–571. doi:10.1093/petrology/egp082

Liu, Y., Hu, Z., Zong, K., Gao, C., Gao, S., Xu, J., et al. (2010b). Reappraisement and refinement of zircon U-Pb isotope and trace element analyses by LA-ICP-MS. *Chin. Sci. Bull.* 55 (15), 1535–1546. doi:10.1007/s11434-010-3052-4

Liu, Y. S., Hu, Z. C., Gao, S., Günther, D., Xu, J., Gao, C. G., et al. (2008). *In situ* analysis of major and trace elements of anhydrous minerals by LA-ICP-MS without applying an internal standard. *Chem. Geol.* 257 (1–2), 34–43. doi:10.1016/j.chemgeo.2008.08.004

Ludwig, K. R. (2003). *Isoplot 3.00: A geochronological toolkit for microsoft excel*. Berkeley, California: Berkeley Geochronology Center.

Qian, T. (2015). Stratigraphic framework of the northern Yangtze foreland basin in the early-middle jurassic: A record of continent-continent collision. PhD dissertation. Beijing: China University of Geosciences.

Qu, H. J., Dong, Y. P., Ma, Q., Zha, X. F., and Xu, Z. Y. (2009). Reversion of paleocurrent directions and its tectonic significance in the late triassic and jurassic period in yunyang chongqing. *J. Northwest Univ. Nat. Sci. Ed.* 39 (3), 528–532.

Shen, Z. Y., Xiao, A. C., Wang, L., Guo, J., Wei, G. Q., and Zhang, L. (2010). Unconformity in the lower triassic of micangshan area, northern sichuan Province: its discovery and significance. *Acta Petrol. Sin.* 26 (4), 1313–1321.

Shi, Y., Yu, J. H., and Santosh, M. (2013). Tectonic evolution of the qinling orogenic belt, Central China: new evidence from geochemical, zircon U-Pb geochronology and Hf isotopes. *Precambrian Res.* 231 (1), 19–60. doi:10.1016/j.precamres.2013.03.001

Sun, D. (2014). The structural character and meso-cenozoic evolution of Micangshan Mountain structural zone, northern Sichuan Basin. PhD dissertation. China: Chengdu University of Technology.

Sun, W. D., Li, S. G., Chen, Y. D., and Li, Y. J. (2000). Zircon U-Pb dating of granitoids from South Qinling, Central China and their geological significance. *Geochimica* 29 (3), 209–216.

Wang, R., Hu, Z., Long, S., Liu, G., Zhao, J., Dong, L., et al. (2019). Differential characteristics of the upper ordovician-lower silurian wufeng-longmaxi shale reservoir and its implications for exploration and development of shale gas in/around the Sichuan Basin. *Acta Geol. Sin. Engl. Ed.* 93 (3), 520–535. doi:10.1111/1755-6724.13875

Xie, J. Q. (2014). Formation age and composite evolution of nappe structure in North Dabashan Mountain. PhD dissertation. Evanston, Illinois: Northwestern University.

Yang, Y. M., Wang, X. J., and Chen, S. L. (2022). Sedimentary system evolution and sandbody development characteristics of Jurassic Shaximiao Formation in the central Sichuan Basin. *Nat. Gas. Ind.* 42 (1), 12–24.

Zhai, M. G., and Bian, A. G. (2000). Late neoarchean supercontinent assembly and late paleoproterozoic-mesoproterozoic breakup in the North China craton. *Sci. China (Series D)* 30, 129–137.

Zhang, G. W., Yu, Z. P., Dong, Y. P., and Yao, A. P. (2000). On precambrian framework and evolution of the qinling. *Acta Petrol. Sin.* 16 (1), 11–21.

Zhang, G. W., Zhang, B. R., Yuan, X. C., and Xiao, Q. H. (2001). *Qinling orogenic belt and continental dynamics*. Beijing: Science Press, 1–855.

Zhang, S. G., Zhang, Z. Q., Song, B., Tang, S. H., Zhao, Z. R., and Wang, J. H. (2005). On the existence of neoarchean materials in the douling Complex,Eastern qinling-evidence from U-Pb SHRIMP and Sm-Nd geochronology. *Acta Geol. Sin.* 78 (6), 800–806.

Zhang, X., Xu, X. Y., Song, G. S., Wang, H. L., Chen, J. L., and Li, T. (2010). Integrative genome-wide approaches in embryonic stem cell research. *Geol. Bull. China* 29 (4), 510–516. doi:10.1039/c0ib00068j

Zhang, Z. Q., Zhang, G. W., Tang, S. H., Zhang, Q. D., and Wang, J. H. (2000). The age of the Hannan intrusive complex and its cause of rapid condensation. *Chin. Sci. Bull.* 45 (23), 2567–2571.

Zhao, F. Q., Zhao, W. P., Zuo, Y. C., Li, Z. H., and Xue, K. Q. (2006). U-Pb geochronology of neoproterozoic magematic rocks in hanzhong, southern shaanxi, China. *Geol. Bull. China* 25 (3), 383–388.

Zhao, J. H., Zhou, M. F., Yan, D. P., Yang, Y. H., and Sun, M. (2008). Zircon Lu-Hf isotopic constraints on Neoproterozoic subduction-related crustal growth along the western margin of the Yangtze Block, South China. *Precambrian Res.* 163 (3–4), 189–209. doi:10.1016/j.precamres.2007.11.003